A SIMPLIFIED NONLINEAR ANALYSIS PROCEDURE FOR SINGLE-STORY ASYMMETRIC BUILDINGS

Kenji FUJII[1], Yoshiaki NAKANO[2], and Yasushi SANADA[3]

[1]Member of JAEE, Post-Doctoral Research Fellow, Dr. Eng., Institute of Industrial Science,
The University of Tokyo, Tokyo, Japan, kfujii@iis.u-tokyo.ac.jp
[2]Member of JAEE, Associate Professor, Dr. Eng., Institute of Industrial Science,
The University of Tokyo, Tokyo, Japan, iisnak@iis.u-tokyo.ac.jp
[3]Member of JAEE, Research Associate, Dr. Eng., Earthquake Research Institute,
The University of Tokyo, Tokyo, Japan, ysanada@eri.u-tokyo.ac.jp

ABSTRACT: A simplified nonlinear analysis procedure to predict earthquake responses of single-story asymmetric buildings is presented and its applicability is discussed. In this procedure, their responses are predicted through a nonlinear static analysis of MDOF model and a nonlinear dynamic analysis of equivalent SDOF model, considering the change in the first mode shape at each nonlinear stage and the effect of the first and second mode contribution. The results show that the responses of torsionally stiff buildings can be satisfactorily predicted by the proposed procedure.

KEY WORDS: asymmetric buildings, equivalent Single-Degree-Of-Freedom (SDOF) model, torsionally stiff (TS) building, torsionally flexible (TF) building, equivalent modal mass ratio

INTRODUCTION

The estimation of nonlinear response of buildings subjected to a strong ground motion is a key issue for the rational seismic design of new buildings and the seismic evaluation of existing buildings (ATC-40 1996, FEMA-273 1997). For this purpose, a nonlinear time-history analysis of Multi-Degree-Of-Freedom (MDOF) model might be one solution, but it is often too complicated whereas the results are not necessarily more reliable due to uncertainties involved in input data. To overcome such shortcomings, several researchers have developed simplified nonlinear analysis procedures (Saiidi and Sozen 1981, Fajfar 2000, Kuramoto et al. 2000). This approach is a combination of a nonlinear static (pushover) analysis of MDOF model and a nonlinear dynamic analysis of the equivalent Single-Degree-Of-Freedom (SDOF) model, and it would be a promising candidate as long as buildings oscillate predominantly in the first mode. Although the simplified procedures have been more often applied to planar frame analyses, some researchers have tried to extend them to multi-story asymmetric buildings (Moghadam and Tso 1996, Azuhata et al. 2000, Fajfar 2002). However, there still include some problems in the simplified procedure for asymmetric buildings: (1) the higher mode response may not be negligible in an asymmetric building, therefore the equivalent SDOF model may not be applicable to some buildings. However few investigations concerning the application limit have been made. (2) To predict the drift demand at each frame from

the pushover analyses of MDOF model, the reasonable force distributions are needed. Since the effect of the second mode contribution may be significant for the drift demand at each frame, the force distribution should be chosen considering the second mode contribution. Although some researchers have tried the applicability of the pushover analysis to predict the drift demand of asymmetric buildings (Moghadam and Tso 1998, Kilar and Fajfar 2001), few rational force distributions are proposed.

To understand the fundamental response characteristics of asymmetric buildings and to clarify the applicability of the simplified procedure to predict their response using equivalent SDOF model, this paper discusses the behavior of single-story asymmetric buildings focusing on (1) the index for the first modal contribution to overall responses, (2) comparison of the equivalent SDOF model responses with MDOF results, and (3) the rational force distributions to predict drift demands at each frame. Based on these discussions, a new simplified procedure is proposed. The proposed procedure in this paper is the combination of a pushover analysis of MDOF model and a nonlinear analysis of the equivalent SDOF model as is in the previous studies (Fajfar 2002), but the change in the first mode shape for the equivalent SDOF model and the effect of the second mode contribution for the pushover analysis of MDOF model are taken into account. This discussion made in this paper is the basis to predict the earthquake response of multi-story asymmetric building with simplified procedure, and the applicability of the proposed procedure to multi-story asymmetric buildings will be discussed elsewhere.

BUILDING AND GROUND MOTION DATA

Building Data

Buildings investigated in this paper are idealized single-story asymmetric buildings: they are assumed to be symmetric about the X-axis as shown in Fig. 1. Their story height H is 3.75m. In this study, eight analytical models are studied considering following parameters: **(1) type of structural plan, (2) moment of inertia, and (3) characteristics of transverse frames**.

(1) Type of structural plan: Two structural plans are studied as shown in Fig. 1. In each model, the column and wall element are placed in frame X1, while only column elements are placed in other frames. Yield strength of each element in two models are shown in Table 1. The yield strengths V_0 in Y-direction of all models are 0.5W (50 % of the total building weight W). All transverse frames of each

(a) Model-1

(b) Model-2

G : Center of Mass
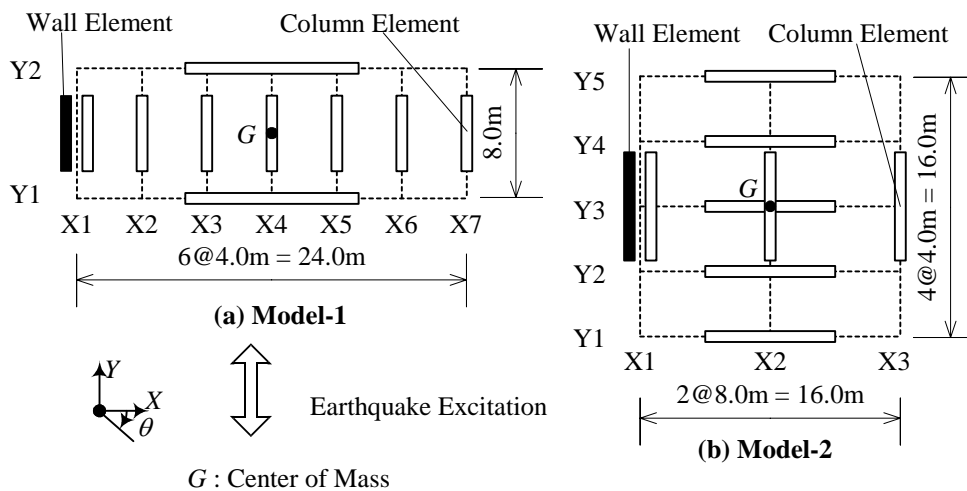
Note: Frame X1 - X7: longitudinal frame, Frame Y1 - Y5: transverse frame

Fig. 1 Plan of the model buildings

2

Table 1 Yield strength of elements in analytical model

	Frame	Yield Strength of Element		Yield Strength of Frame
		Column Element	Wall Element	
Model-1	X1	0.050W	0.150W	0.200W
	X2 - X7			0.050W
	Y1, Y2			(0.250W)
Model-2	X1	0.117W	0.150W	0.267W
	X2, X3			0.117W
	Y1 – Y5			(0.100W)

Note: The yield strengths V_0 of all models in Y-direction and those of all N-Series models in X-Direction are assumed 0.5W (50 % of the total building weight W).

(a) Column Element   **(b) Wall Element**   **(c) Transverse Frame**

**Note:** α_y is determined from K_E, V_y, and D_y.
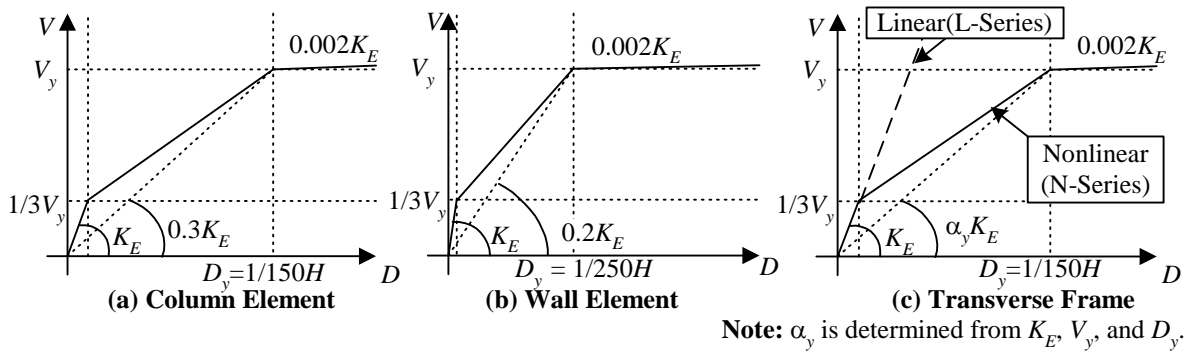
Fig. 2 Envelopes of restoring force-displacement relationship

model are identical and the elastic stiffness in X-direction of the whole building is assumed identical with that in Y-direction. Both models are symmetric about the X-axis.

Fig. 2 shows the envelope curve of restoring force-displacement relationship of each element. The envelopes are assumed symmetric in both positive and negative loading directions. The Takeda hysteretic model (Takeda et al. 1970) is employed for both column and wall elements, assuming that they behave in a ductile manner.

(2) Moment of inertia: Several studies within the elastic range have shown that the responses of asymmetric buildings are significantly influenced by the ratio of uncoupled torsional frequency to

(a) Model-TS Series   **(b) Model-TF Series**
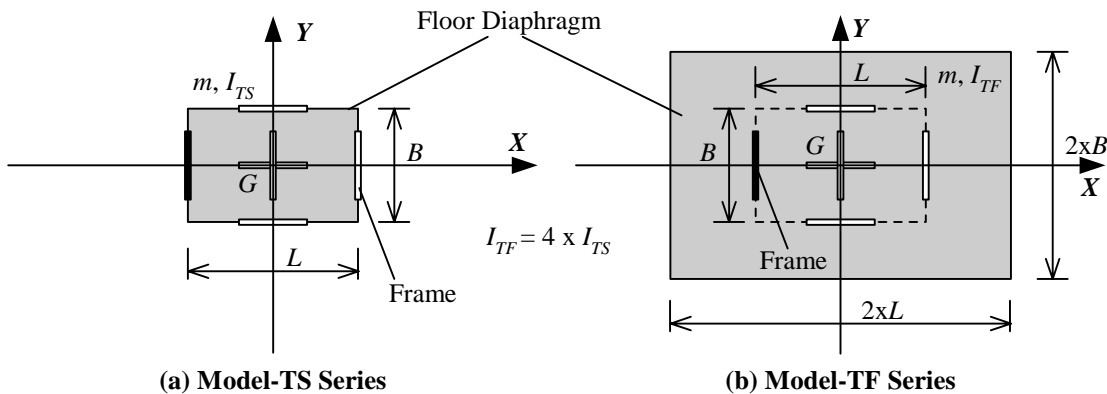
Note: m: mass, I_{TS}, I_{TF}: Moment of Inertia of Model-TS/TF Series

Fig. 3 Moment of inertia of Model-TS/TF Series

uncoupled translational frequency (Kan and Chopra 1977, Yamazaki 1988, Ohami and Murakami 2000). To investigate the influence of the frequency ratio on the nonlinear responses of asymmetric buildings, two structural series as shown in Fig. 3 are considered.

Model-TS Series: The unit mass is assumed 1.2 x 10^3kg/m^2. The ratio of uncoupled torsional frequency to uncoupled translational frequency is larger than 1.

Model-TF Series: The moment of inertia I is assumed four times as large as that of Model-TS series, while the total mass m is same as Model-TS series: in the TF series, the dimensions of floor diaphragm is twice as large as that of Model-TS series, while the unit mass is one-forth of Model-TS series as shown in Fig. 3(b). The locations of all frames are the same as Model-TS series. The radius of gyration of floor r is defined as Eq. (1).

$$r = \sqrt{I/m} \tag{1}$$

It should be pointed out that r is twice as large as that of Model-TS series. The ratio of uncoupled torsional frequency to uncoupled translational frequency is less than 1.

(3) Characteristics of transverse frames: To discuss the influence of the stiffness degradation in the transverse frames on the applicability of the simplified procedure, two cases are studied as shown in Fig. 2(c) for each model.

Model-L Series: The transverse frames are assumed linear. This series corresponds to the buildings of which transverse frames have much larger strength than longitudinal frames as Japanese typical R/C school buildings, due to the presence of shear walls in transverse frames.

Model-N Series: The transverse frames are assumed nonlinear. The yield strengths V_0 in X-direction of these models are 0.5W; therefore these models have the same strength in both directions.

Input ground motions

In this study, the earthquake excitation is considered unidirectional in Y-direction, and the following six ground motions are used: the NS component of the El Centro record obtained during the 1940 Imperial Valley earthquake (referred to as ELC), the NS component of the Taft record obtained during the 1952 California earthquake (TAF), the EW component of the Hachinohe record obtained during the 1968 Tokachi-Oki earthquake (HAC), the NS component of the Tohoku University record obtained during the 1978 Miyagiken-oki earthquake (TOH), the NS component of the Kobe Meteorological Observatory record and the NS component of the Fukiai record obtained during 1995 Hyogo-ken Nanbu Earthquake (KMO and FKI, respectively). The first 25 seconds of each record are used in this study. All ground motions are scaled so that the maximum drift of a Takeda SDOF model having the yield strength of 0.5W reach the drift angle of 1/100. The normalized absolute acceleration response
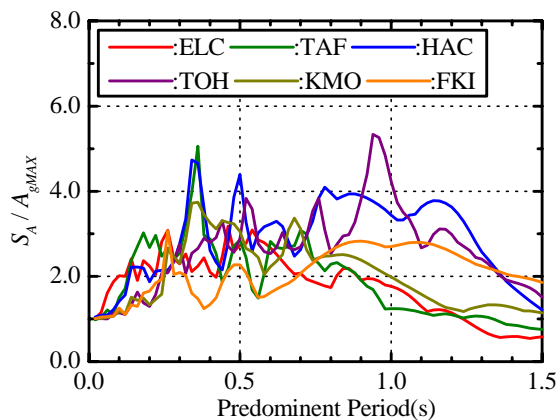

Fig. 4 Normalized acceleration response spectra

Table 2 List of ground motion

Ground Motion Record ID	Original PGA (m/s^2)	Amplification Factor
ELC	3.417	1.079
TAF	1.572	2.452
HAC	1.829	1.423
TOH	2.582	0.994
KMO	8.178	0.398
FKI	8.020	0.561

4

spectra with 3% critical damping for 6 ground motions are shown in Fig. 4. Table 2 shows the original PGA and amplification factor for all ground motions.

Numerical analysis procedure

In this study, the damping matrix is assumed proportional to the instant stiffness matrix and 3% of the critical damping for the first mode. Newmark-β method $(\beta = 1/4)$ is applied in numerical integrations. The time increment for numerical integration is 0.005 sec. The unbalanced force due to stiffness change is corrected at a next time step during analysis.

TORSIONALLY STIFF BUILDINGS AND TORSIONALLY FLEXIBLE BUILDINGS

In this chapter, the asymmetric building models are classified based on their dynamic characteristics. The equation of motion of undamped free vibration of single-story asymmetric buildings can be written as Eq. (2). Since the asymmetric buildings considered in this paper are symmetric about X-axis and the earthquake excitation is considered unidirectional in Y-Direction, only 2 degrees of freedom (displacement at the center of mass in Y-direction y and rotational angle θ) are considered in Eq. (2).

$$\begin{bmatrix} m & 0 \\ 0 & I \end{bmatrix} \begin{Bmatrix} \ddot{y} \\ \ddot{\theta} \end{Bmatrix} + \begin{bmatrix} K_Y & -K_Y \cdot e_K \\ -K_Y \cdot e_K & K_\theta \end{bmatrix} \begin{Bmatrix} y \\ \theta \end{Bmatrix} = \begin{Bmatrix} 0 \\ 0 \end{Bmatrix} \tag{2}$$

where $[M] = \begin{bmatrix} m & 0 \\ 0 & I \end{bmatrix}$: mass matrix, $[K] = \begin{bmatrix} K_Y & -K_Y \cdot e_K \\ -K_Y \cdot e_K & K_\theta \end{bmatrix}$: elastic stiffness matrix, $\{d\} = \{y \quad \theta\}^T$: vector representing displacement at the center of mass and rotation, m: mass, I: moment of inertia, K_Y: elastic lateral stiffness in Y-direction, $K_\theta = K_Y \cdot j^2$: elastic torsional stiffness with respect to the center of mass, e_K: elastic eccentricity, j: radius of gyration of story stiffness with respect to the center of mass. By substituting Eqs. (3) and (4) into Eq. (2), Eq. (5) is obtained.

$$z = r \cdot \theta, \quad E = e_K / r, \quad J = j/r \tag{3}$$

$$\omega_{0Y} = \sqrt{K_Y/m}, \quad \omega_{0\theta} = \sqrt{K_\theta/I} = (j/r) \cdot \sqrt{K_Y/m} = J \cdot \omega_{0Y} \tag{4}$$

$$\begin{Bmatrix} \ddot{y} \\ \ddot{z} \end{Bmatrix} + \omega_{0Y}^2 \begin{bmatrix} 1 & -E \\ -E & J^2 \end{bmatrix} \begin{Bmatrix} y \\ z \end{Bmatrix} = \begin{Bmatrix} 0 \\ 0 \end{Bmatrix} \tag{5}$$

where E is the eccentricity ratio, J is the radius ratio of gyration of story stiffness, ω_{0Y} and $\omega_{0\theta}$ are the uncoupled translational frequency and uncoupled torsional frequency, respectively. Note that J equals the ratio of uncoupled torsional frequency to uncoupled translational frequency as shown in Eq. (4) (Ohami and Murakami 2000). The i-th natural frequency ω_i and i-th mode shape vector $\{\phi_i\} = \{\phi_{Yi}, \phi_{Zi}\}^T$ of the single-story asymmetric building models can be obtained from Eq. (5) as shown in Eqs. (6) and (7).

$$\begin{aligned} \omega_1^2 \\ \omega_2^2 \end{aligned} \Bigg\} = \frac{(1+J^2) \mp \sqrt{(1-J^2)^2 + 4E^2}}{2} \cdot \omega_{0Y}^2 \tag{6}$$

$$\phi_{Yi}/\phi_{Z_i} = \left\{ J^2 - (\omega_i/\omega_{0Y})^2 \right\} / E \tag{7}$$

Fig. 5 shows the definition of torsionally stiff (TS) buildings and torsionally flexible (TF) buildings. In this figure, the distance from the center of mass G to the center of rotation of i-th mode O_i is obtained
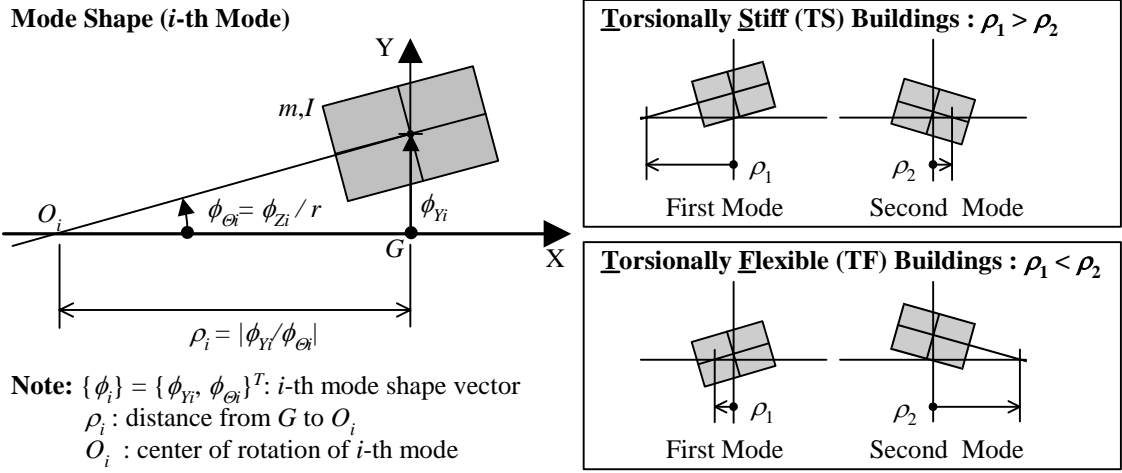
Fig. 5 Definition of torsionally stiff (TS) building and torsionally flexible (TF) building

by Eq. (8).

$$\rho_i = \left|\phi_{Yi}/\phi_{\Theta i}\right| = r \cdot \left|\phi_{Yi}/\phi_{Zi}\right| \tag{8}$$

In this study, the building model is classified as TS building when ρ_1 is larger than ρ_2, and it is classified as TF buildings when ρ_1 is smaller than ρ_2. By substituting Eq. (7) into Eq. (8), Eq. (9) can be obtained.

$$\rho_i/r = \left|\left\{J^2 - (\omega_i/\omega_{0Y})^2\right\}/E\right| \tag{9}$$

Eq. (10) is obtained from Eqs. (6) and (9).

$$
\begin{aligned}
(\rho_1/r)^2 - (\rho_2/r)^2 &= \left\{(\omega_2/\omega_{0Y})^2 - (\omega_1/\omega_{0Y})^2\right\}\left[2J^2 - \left\{(\omega_1/\omega_{0Y})^2 + (\omega_2/\omega_{0Y})^2\right\}\right]/E^2 \\
&= \left\{(\omega_2/\omega_{0Y})^2 - (\omega_1/\omega_{0Y})^2\right\}(J^2 - 1)/E^2 \\
&\quad \left(\because (\omega_1/\omega_{0Y})^2 + (\omega_2/\omega_{0Y})^2 = 1 + J^2\right)
\end{aligned}
\tag{10}
$$
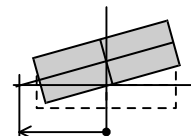
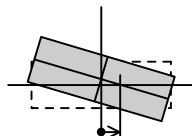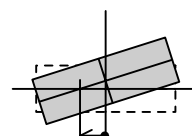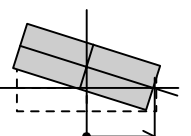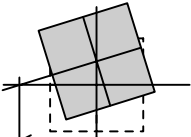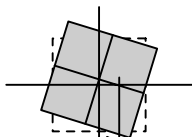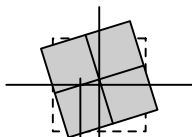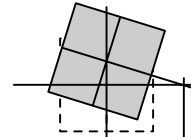In Eq. (10), $(\omega_2/\omega_{0Y})^2 - (\omega_1/\omega_{0Y})^2 > 0$ because $\omega_2 > \omega_1$. Therefore the relationship of ρ_1 and ρ_2 is expressed as Eq. (11).

$$
\begin{cases}
\rho_1 < \rho_2 & \text{for } J < 1 \\
\rho_1 = \rho_2 & \text{for } J = 1 \\
\rho_1 > \rho_2 & \text{for } J > 1
\end{cases}
\tag{11}
$$

Eq. (11) reveals the buildings with $J > 1$ are classified as TS buildings, while those with $J < 1$ are classified as TF buildings. Table 3 shows the model parameters: E, J, and eccentricity ratio in

Table 3 Model parameters

Torsionally Stiff (TS) Buildings				Torsionally Flexible (TF) Buildings			
	E	J	Re		E	J	Re
Model-1-TS-L/N	0.850	1.509	0.682	Model-1-TF-L/N	0.425	0.755	0.682
Model-2-TS-L/N	0.634	1.418	0.500	Model-2-TF-L/N	0.317	0.709	0.500

Torsionally Stiff Buildings(TS)			Torsionally Flexible Buildings(TF)		
	First Mode	Second Mode		First Mode	Second Mode
Model-1-TS-L/N	$\rho_1 / r = 2.000$	$\rho_2 / r = 0.500$	Model-1-TF-L/N	$\rho_1 / r = 0.614$	$\rho_2 / r = 1.629$
	$T_1 = 0.269$s	$T_2 = 0.124$s		$T_1 = 0.368$s	$T_2 = 0.182$s
Model-2-TS-L/N	$\rho_1 / r = 2.075$	$\rho_2 / r = 0.482$	Model-2-TF-L/N	$\rho_1 / r = 0.486$	$\rho_2 / r = 2.058$
	$T_1 = 0.245$s	$T_2 = 0.134$s		$T_1 = 0.346$s	$T_2 = 0.190$s

Note: r: radius of gyration of floor, T_1, T_2: natural periods of the first and second mode, respectively.

Fig. 6 Mode shapes and natural periods of analytical models

accordance with Japanese Standard of Seismic Design of Buildings *Re*, and Fig. 6 shows the natural periods and mode shapes of each model. They show that Model-TS series are classified in TS buildings, while Model-TF series are classified in TF buildings. Table 3 also shows that *Re* of all building models is larger than 0.3 and therefore these building models have extremely large eccentricity. It should be pointed out that *Re* of TF buildings are same as those of TS buildings. This indicates that the influence of the frequency ratio on the dynamic characteristics of asymmetric buildings is *not* taken into account in *Re*.

EQUIVALENT SDOF MODEL

The equation of motion of a single-story asymmetric building model can be expressed as Eq. (12).

$$[M]\{\ddot{d}\} + [C]\{\dot{d}\} + \{R\} = -[M]\{\alpha\} \cdot a_g \tag{12}$$

where $[C]$: damping matrix, $\{R\} = \{V_Y \quad T_Z\}^T$: vector representing restoring forces(shear force and torque at the center of mass), $\{\alpha\} = \{1 \quad 0\}^T$: vector defining the direction of ground motion, a_g: ground acceleration.

The displacement and restoring force vectors are assumed in the form of Eq. (13) even if the building responds beyond the elastic range.

$$\{d\} = \{d_1\} + \{d_2\}, \quad \{R\} = \{R_1\} + \{R_2\} \tag{13}$$

$$\{d_i\} = \Gamma_i \{\phi_i\} \cdot D_i^*, \quad \{R_i\} = \Gamma_i [M]\{\phi_i\} \cdot A_i^* \tag{14}$$

$$\Gamma_i = \frac{\{\phi_i\}^T [M]\{\alpha\}}{\{\phi_i\}^T [M]\{\phi_i\}} \tag{15}$$

where $\{d_i\}$: i-th modal displacement, $\{R_i\}$: i-th modal restoring force, D_i^*: i-th modal equivalent displacement, A_i^*: i-th modal equivalent acceleration, Γ_i: i-th modal participation factor.

Note that the mode shape vector $\{\phi_i\}$ *varies* depending on the stiffness degradation. In this study, $\{\phi_i\}$

is determined from the secant stiffness defined at the maximum deformation previously experienced in the calculation.

D_i^* and A_i^* can be rewritten as Eq. (16) from Eqs. (13) through (15).

$$D_i^* = \Gamma_i \{\phi_i\}^T [M]\{d\}/M_i^*, \quad A_i^* = R_i^*/M_i^* = \Gamma_i \{\phi_i\}^T \{R\}/M_i^* \tag{16}$$

$$M_i^* = \Gamma_i^2 \left(\{\phi_i\}^T [M]\{\phi_i\}\right) \tag{17}$$

where: M_1^*: i-th modal equivalent mass, $R_i^* = \Gamma_i \{\phi_i\}^T \{R\}$: i-th modal equivalent restoring force.

Assuming that the predominant first mode oscillation and neglecting the second mode of the building, Eq. (13) can be rewritten as Eq. (18).

$$\{d\} = \Gamma_1\{\phi_1\} \cdot D_1^*, \quad \{R\} = \Gamma_1 [M]\{\phi_1\} \cdot A_1^* \tag{18}$$

By substituting Eq. (18) into Eq. (12) and by multiplying $\Gamma_1\{\phi_1\}^T$ from the left side, the equation of motion of the equivalent SDOF model is obtained as Eq. (19).

$$\ddot{D}_1^* + \frac{C_1^*}{M_1^*} \cdot \dot{D}_1^* + A_1^* = -a_g \tag{19}$$

where C_1^* is the first modal equivalent damping coefficient defined by Eq. (20).

$$C_1^* = \Gamma_1^2 \left(\{\phi_1\}^T [C]\{\phi_1\}\right) \tag{20}$$

APPLICABILITY OF THE EQUIVALENT SDOF MODEL

The equivalent SDOF model described in the previous chapter is fundamentally based on the assumption that buildings oscillate predominantly in the first mode throughout the responses. In this chapter, the applicability of the model to asymmetric buildings is discussed focusing on: (1) the equivalent modal mass ratio representing the modal contribution to overall response, (2) comparisons of the modal responses between TS and TF buildings, and (3) comparison of responses between the equivalent SDOF model and MDOF model.

Equivalent modal mass ratio

To understand the first modal contribution to overall response, the equivalent modal mass ratio m_i^* defined by Eq. (21) is employed.

$$m_i^* = M_i^*/m = \Gamma_i^2 \left(\{\phi_i\}^T [M]\{\phi_i\}\right)/m \tag{21}$$

The equivalent modal mass ratio m_i^* varies from 0 to 1 and the sum for all modes is unity. When m_1^* is equal to 1.0, the response of the MDOF model is governed totally by its first mode. The equivalent modal mass ratio m_1^* therefore can be a good index for the first modal contribution to overall response. Eq. (17) can be rewritten as Eq. (22) from Eqs. (1), (8) and (15).

$$M_i^* = \frac{\left(\{\phi_i\}^T [M]\{\alpha\}\right)^2}{\{\phi_i\}^T [M]\{\phi_i\}} = \frac{\phi_{Yi}^2}{\phi_{Yi}^2 + (r \cdot \phi_{\Theta i})^2} \cdot m = \frac{1}{1 + (r/\rho_i)^2} \cdot m \tag{22}$$
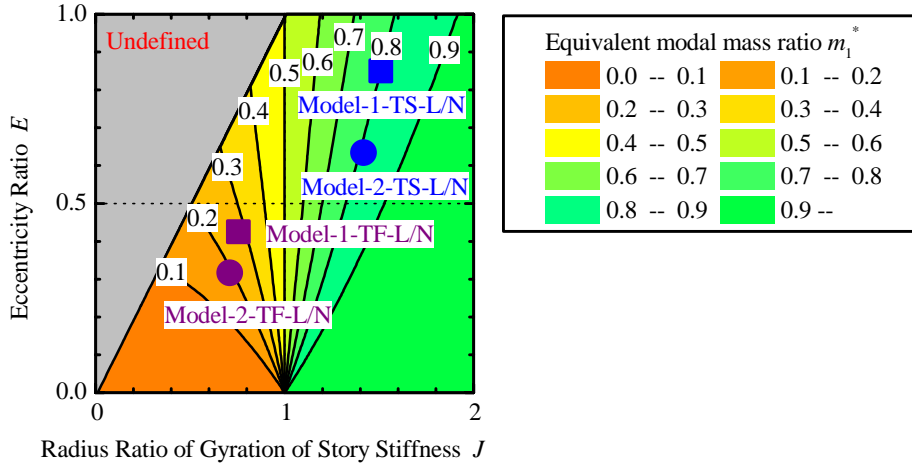
Fig. 7 contour line of m_1^* on the E-J plane

Substituting Eq. (22) into Eq. (21), Eq. (23) is obtained.

$$m_i^* = \frac{1}{1+\left(r/\rho_i\right)^2} \tag{23}$$

Eq. (23) indicates that m_1^* equals 1 when the first mode response is purely translational ($\rho_1 = \infty$), while m_1^* equals 0 when the first mode response is purely torsional ($\rho_1 = 0$). This equation also indicates that m_1^* is larger than m_2^* for TS buildings ($\rho_1 > \rho_2$), while m_1^* is smaller than m_2^* for TF buildings ($\rho_1 < \rho_2$).

Fig. 7 shows the contour line of m_1^* on the E-J plane. This figure shows that m_1^* is larger than 0.5 for TS buildings ($J > 1$), but smaller than 0.5 for TF buildings ($J < 1$). This implies that TS buildings have relatively large m_1^* value and may respond predominantly in the first mode while TF buildings may be significantly influenced by the second mode.

Modal response contribution to overall response

To investigate the difference of modal response contribution between TS and TF buildings, their time-history responses are decomposed into "modal" components. The decomposition procedure is summarized below in a step-by-step form:

1) Carry out a nonlinear time-history analysis of MDOF model.
2) Determine the equivalent stiffness of element at each step from the time-history response analysis. In this study, the equivalent stiffness of each element is defined by its secant stiffness at the maximum deformation previously experienced.
3) Determine the mode shapes $\Gamma_i\{\phi_i\}(i=1,2)$ at each step from the equivalent stiffness.
4) Determine the i-th modal equivalent displacement D_i^* from Eq. (16).
5) Determine the i-th modal displacement $\{d_i\}$ from Eq. (14).

Figs. 8 and 9 show the decomposed displacement at the center of mass y, rotational angle θ for Model-1-TS-L and Model-2-TF-L, respectively, subjected to TOH ground motion.
As can be found in these figures, the first mode response has a high contribution to the overall response in TS building, whereas the second mode response is not negligibly small in TF building. It should be also pointed out that m_1^* is more than 0.8 and stable throughout the response in TS building but it is less than 0.5 for the first 8 sec. and tends to increase monotonically in TF building. These
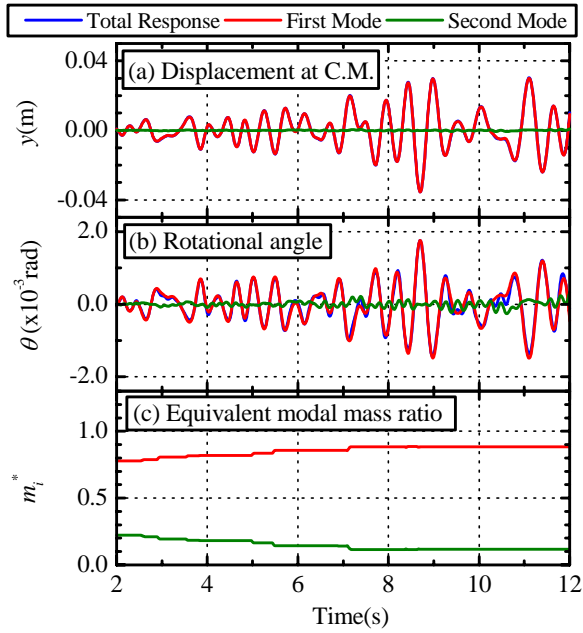
9
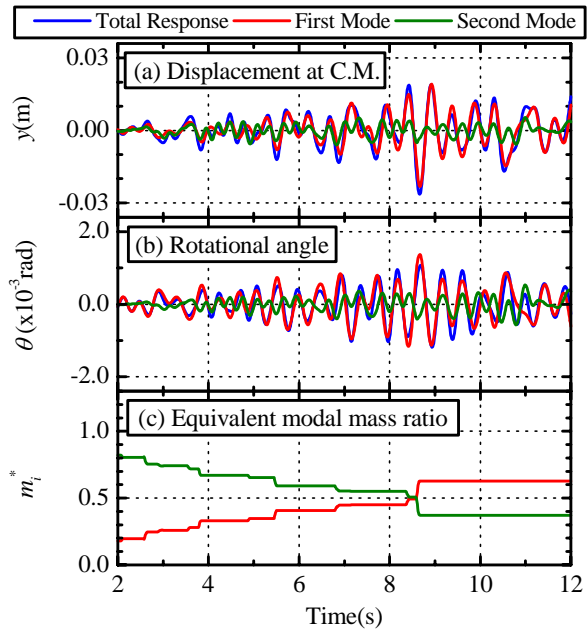
Fig. 8 Modal decomposition (Model-1-TS-L)   Fig. 9 Modal decomposition (Model-2-TF-L)

results conclude that the asymmetric building studied herein oscillates predominantly in the first mode only when it is classified in TS building.

Applicability of equivalent SDOF model to asymmetric buildings

The results obtained in the previous section imply that the equivalent SDOF model can be limitedly applied to the TS buildings that may oscillate predominantly in the first mode. To confirm its applicability, the nonlinear dynamic time-history analysis results of equivalent SDOF models are further compared with those of MDOF models. The detailed numerical analysis procedure can be found in **APPENDIX A**.
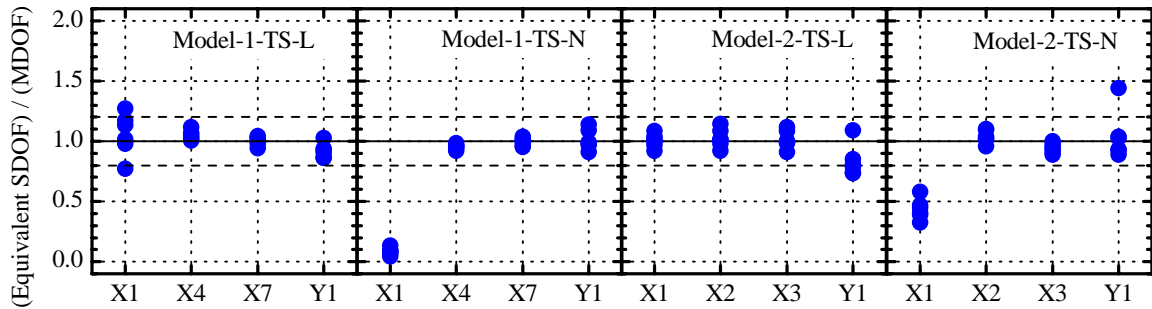

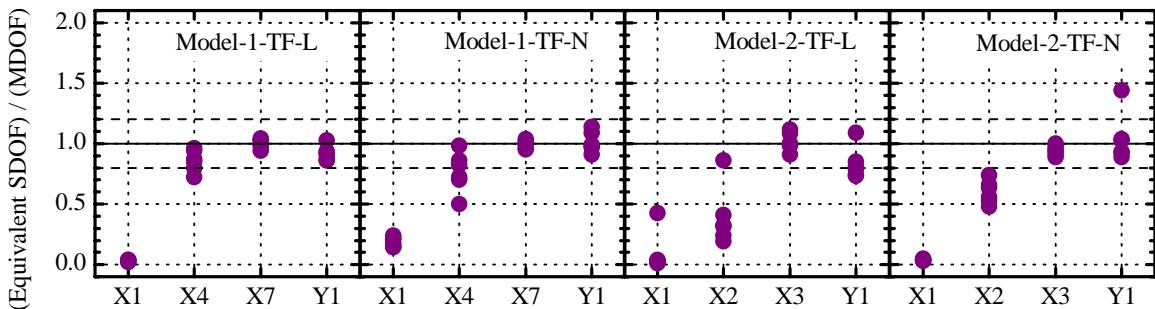Fig. 10 Accuracy of the Equivalent SDOF model (TS Buildings)

Fig. 11 Accuracy of the Equivalent SDOF model (TF Buildings)

10

Figs. 10 and 11 show the ratio of maximum drift at stiff-side frame (Frame X1 for both Model-1 and Model-2), center of mass (Frame X4 for Model-1 and Frame X2 for Model-2, respectively), flexible-side frame (Frame X7 for Model-1 and Frame X3 for Model-2, respectively) and the transverse frame (Frame-Y1 for both Model-1 and Model-2) predicted by the equivalent SDOF model to MDOF model. These figures reveal satisfactory agreement in TS buildings except stiff-side frame in Model-1-TS-N and Model-2-TS-N, but significant difference in TF buildings. The reason why the maximum drift at stiff-side frame is significantly underestimated in Model-1-TS-N and Model-2-TS-N will be discussed later.

To understand the different characteristics between two structural series, the responses of Model-1-TS-L and Model-2-TF-L subjected to TOH ground motion are compared in Figs. 12 and 13. These figures show that the response of the MDOF model and the equivalent SDOF model agrees well in Model-1-TS-L while they differ significantly in Model-2-TF-L. This concludes that the equivalent SDOF model can be limitedly applied to TS buildings. Therefore, the discussion in the following sections will be limited to the TS buildings.

Influence of mode shape change

In the previous section, the applicability of the equivalent SDOF model to the asymmetric building is discussed. However, as can be easily understood from the equation of motion of the equivalent SDOF model, the mode shape assumption is another essential factor to obtain a satisfactory estimation of structural response from the equivalent SDOF model. In the previous discussions of this paper, the first mode shape beyond the elastic range is found from the secant stiffness of elements, and the variable mode shape is taken into account in the nonlinear response analyses. To investigate its influence on the response estimation, the results are compared with those assuming a constant first mode shape based on the elastic stiffness throughout the response.

Fig. 14 compares the response displacement ratio (Equivalent SDOF/MDOF) at the center of mass and rotation for two models, i.e., variable and constant mode shape models. The figure shows a remarkable
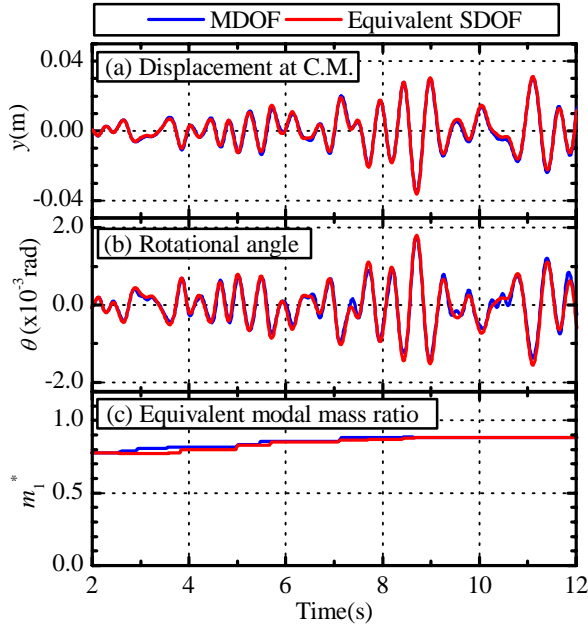

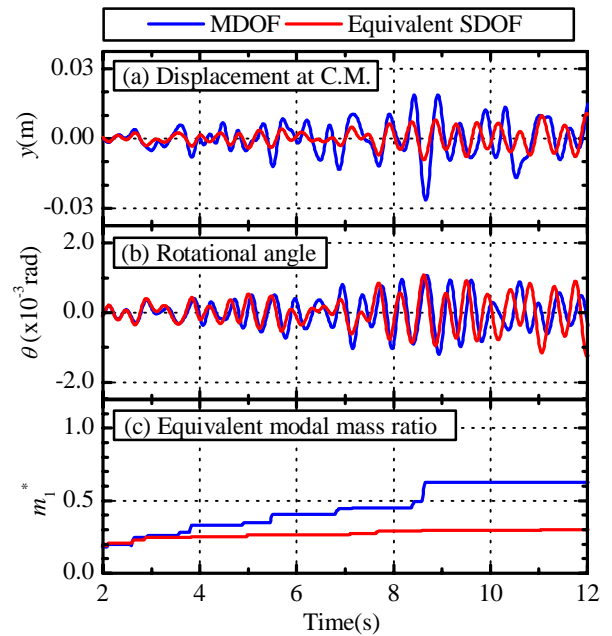Fig. 12 Comparison the equivalent SDOF model and MDOF model (Model-1-TS-L)

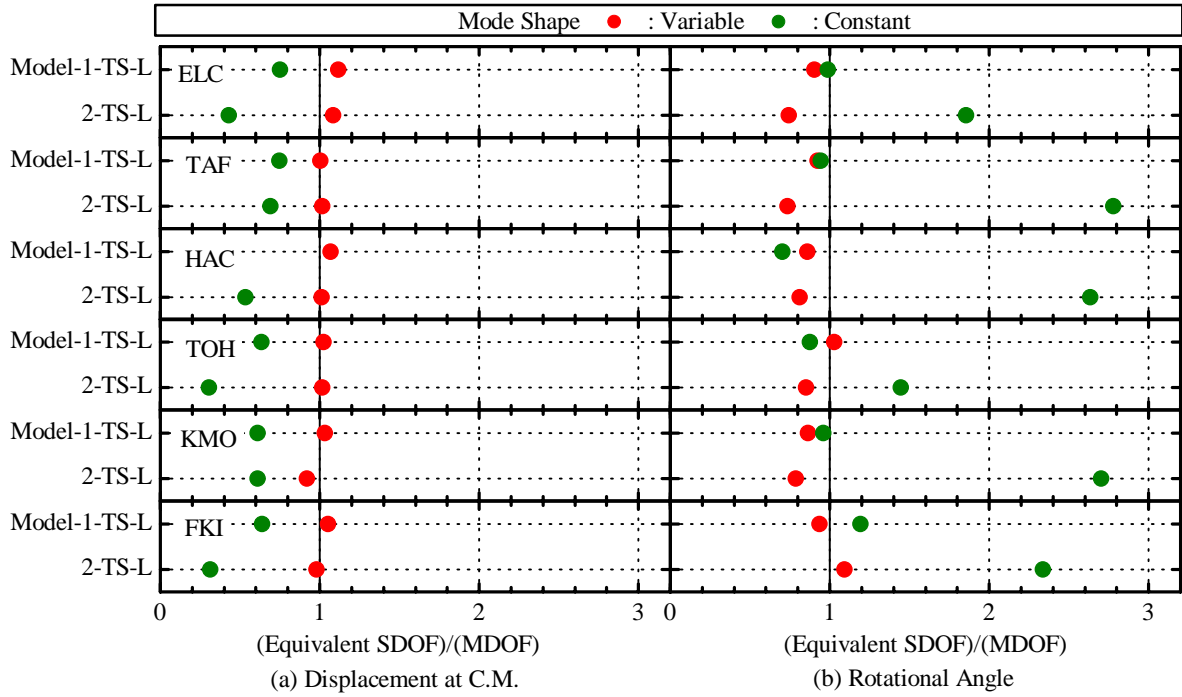Fig. 13 Comparison the equivalent SDOF model and MDOF model (Model-2-TF-L)

(a) Displacement at C.M. (b) Rotational Angle

Fig. 14 Response ratio of the equivalent SDOF model to MDOF model
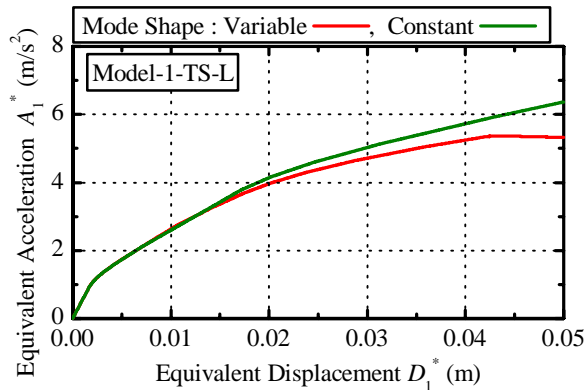

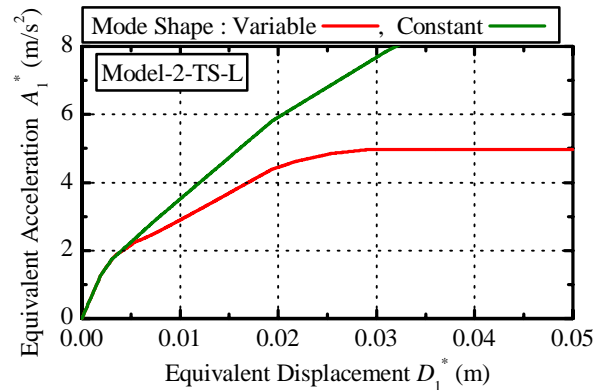Fig. 15 Comparison of A_1^*-D_1^* relationship
(Model-1-TS-L)

Fig. 16 Comparison of A_1^*-D_1^* relationship
(Model-2-TS-L)

difference in two models and the constant mode shape models significantly underestimate the displacement at center of mass and overestimate the rotation obtained by MDOF responses.

Figs. 15 and 16 show the A_1^* - D_1^* relationship of Model-1-TS-L and Model-2-TS-L obtained from the pushover analysis. It shows that A_1^* of the "constant" mode shape model is much larger than that of "variable" model, which is resulted from (1) the underestimated modal equivalent mass M_1^* and (2) the overestimated modal equivalent restoring force R_1^* to calculate A_1^* defined in Eq. (16).
It is therefore essential to incorporate the change in the first mode shape to obtain more accurate responses of asymmetric buildings through the equivalent SDOF models.

PREDICTION OF DRIFT DEMAND USING PUSHOVER ANALYSIS OF MDOF MODEL

Fig. 10 has shown that the equivalent SDOF model underestimates the drift demand at stiff-side frame obtained by MDOF model even for TS buildings (Model-1-TS-N, Model-2-TS-N). The estimation of the drift demand at stiff-side frame may be critical if it consists of brittle elements and the flexible-side

frame consists of ductile elements. As discussed later in detail, this implies that the influence of the second mode contribution may be significant at the stiff-side frame, and therefore it should be considered for a better prediction of the drift demand. Dr. Matsumori et al. proposed a procedure to predict the demands of planar frame structures by pushover analysis using two different force distributions considering the first and second mode contribution (Matsumori et al. 2002). In this chapter, the applicability of that procedure to the asymmetric TS buildings is discussed focusing on: (1) the influence of the stiffness degradation in transverse frames on the response of TS buildings and (2) comparisons of the dynamic analysis results and the pushover analyses results.

Influence of the stiffness degradation in transverse frames on the response of TS buildings

To understand the influence of the stiffness degradation in transverse frames on the nonlinear response of TS buildings, pushover analyses are carried out. In this study, the following assumptions are made to impose displacements on the MDOF model:

1) The equivalent stiffness of elements can be defined by their secant stiffness at a maximum deformation previously experienced in the calculation.
2) The first mode shape at each loading stage can be determined from the equivalent stiffness.
3) The deformation shape imposed on a model is same as the first mode shape obtained in 2).
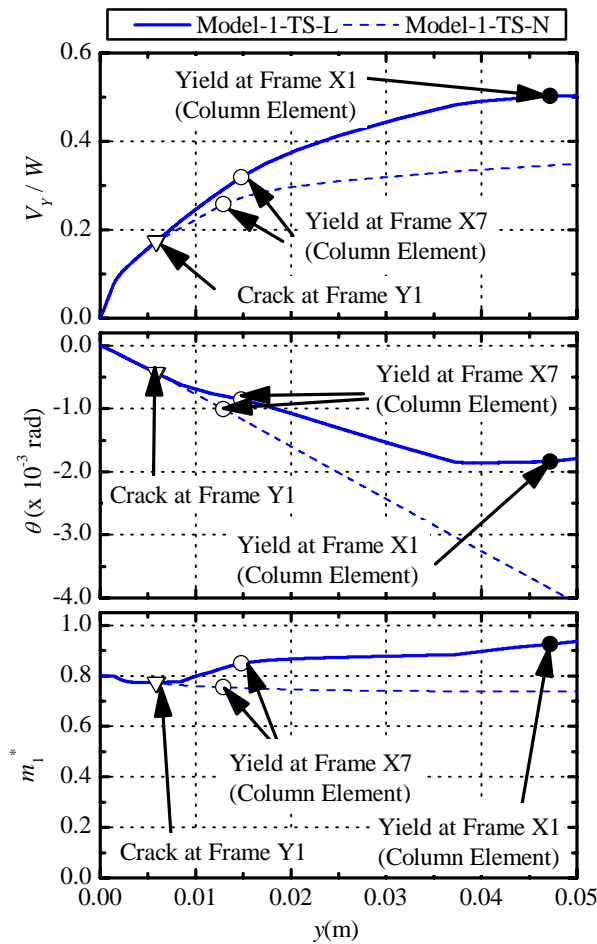
The detailed procedure can be found in **APPENDIX B**.

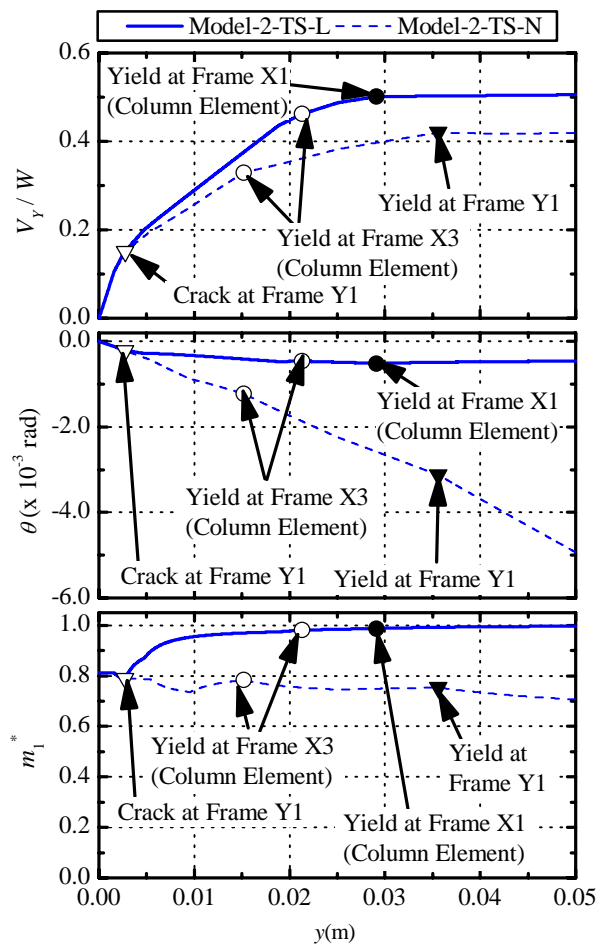Fig. 17 Comparison of the results of pushover analysis (Model-1-TS)

Fig. 18 Comparison of the results of pushover analysis (Model-2-TS)
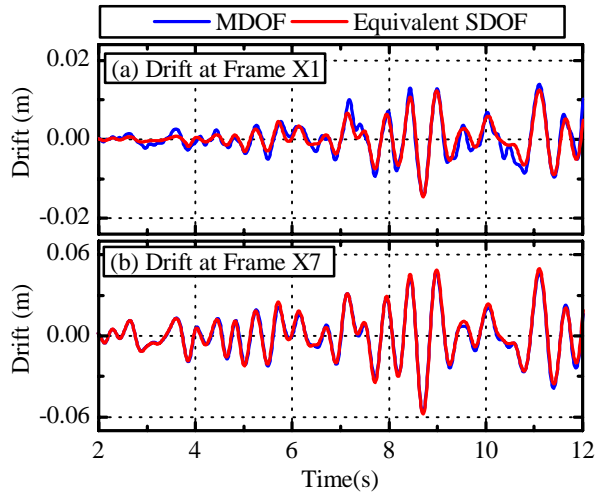
13

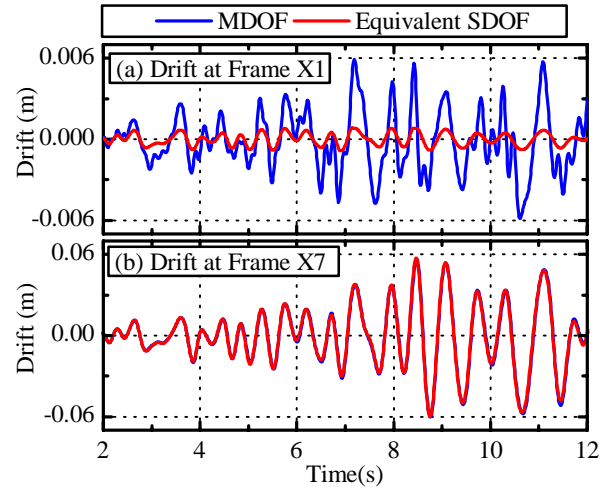Fig. 19 Comparison of the response at Frame X1 and Frame X7 (Model-1-TS-L)

Fig. 20 Comparison of the response at Frame X1 and Frame X7 (Model-1-TS-N)

Figs. 17 and 18 compare the nonlinear characteristics of Model-L (Model-1-TS-L, Model-2-TS-L) and Model-N (Model-1-TS-N, Model-2-TS-N). These figures reveal that the nonlinear characteristics of both series differ significantly. In Model-N series, the rotational angle θ increases almost linearly as the displacement y increases due to the stiffness degradation of the transverse frames while the increase of the rotation is less significant in Model-L series. It should be pointed out that equivalent first modal mass ratio m_1^* increases monotonically in Model-L series, while m_1^* decreases slightly but keeps a value of above 0.7 throughout analysis in Model-N series. This implies that the stiffness degradation of the transverse frames may increase the second mode contribution.

To understand the influence of the stiffness degradation of the transverse frames on dynamic response of TS buildings, the responses of Model-1-TS-L and Model-1-TS-N subjected to TOH ground motion are compared in Figs. 19 and 20. These figures show that the response of the MDOF model and the equivalent SDOF model agrees well at both Frame X1 and Frame X7 in Model-1-TS-L, while they differs significantly at Frame X1 in Model-1-TS-N.

Procedure for estimating drift demand using two different pushover analyses

In this section, the applicability of the procedure proposed by Dr. Matsumori at al. (Matsumori et al. 2002) to the asymmetric TS buildings is discussed.

Fig. 21 shows the concept of the procedure using two different pushover analyses. The outline of the procedure is summarized below:

1)   Pushover Analysis to first mode response (referred to as Pushover-1)
1-1)   Calculate the equivalent displacement $D_1^*{}_{MAX}$ by equivalent SDOF model.
1-2)   Determine the drift demand based on the first mode response from the results of the pushover analysis and $D_1^*{}_{MAX}$ obtained from 1).
2)   Pushover Analysis to sum of modal forces (referred to as Pushover-2)
2-1)   Determine the sum of modal force distribution $\{f\}_+$ from response spectrum.
2-2)   Carry out the pushover analysis using the sum of modal forces until the equivalent displacement D^* reaches $D_1^*{}_{MAX}$ obtained from 1-1).
3)   Determine the drift demand by the envelope of (a) Pushover-1 obtained from 1) and (b) Pushover-2 obtained from 2).

This procedure is applied to asymmetric buildings in this study, while it is originally applied to planar
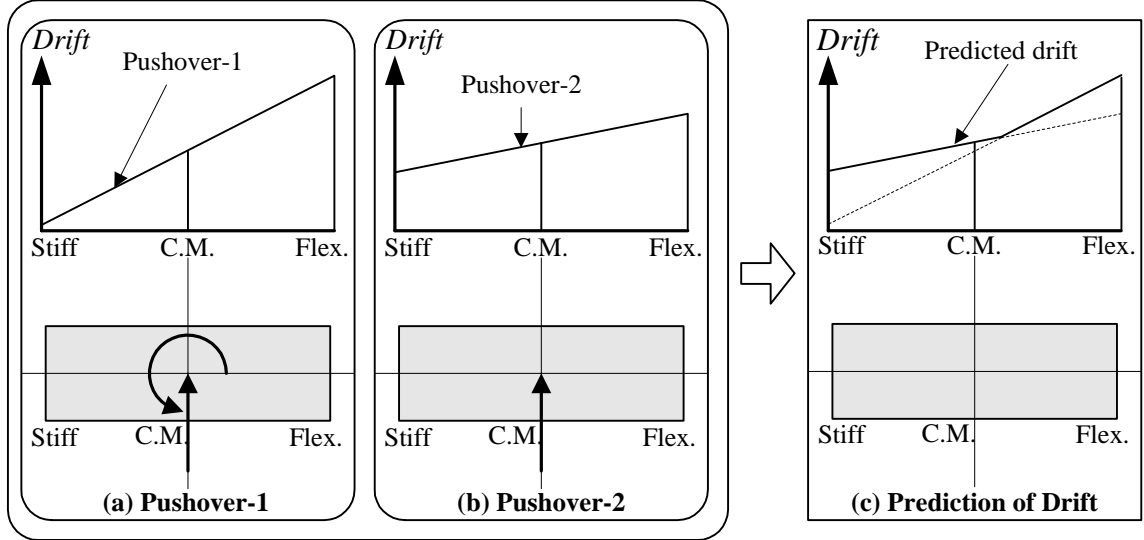
Fig. 21 Concept of the procedure using two different pushover analyses

frames in the previous study (Matsumori et al. 2002). To apply the procedure to asymmetric buildings, the following two modifications are made as described below.

(1) Calculation of equivalent displacement: Since the change of the first mode shape is considered in this study, the equivalent displacement for the pushover analysis using the sum of modal forces distribution D^* is calculated by Eq. (24).

$$D^* = \frac{\Gamma_{1ie}\{\phi_{1ie}\}^T [M]\{d\}}{\Gamma_{1ie}\{\phi_{1ie}\}^T [M]\{\alpha\}} \tag{24}$$

where: $\Gamma_{1ie}\{\phi_{1ie}\}$: first mode shape at $D_1{}^*_{MAX}$. The pushover analysis is carried out until D^* obtained by Eq. (24) reaches $D_1{}^*_{MAX}$.

(2) Determination of the sum of modal force distribution: The sum of modal force distribution $\{f\}_+$ is determined by Eq. (25) (Matsumori et al. 2002).

$$\{f\}_+ = [M](\Gamma_1\{\phi_1\} + \alpha_{2+}\Gamma_2\{\phi_2\}) \tag{25}$$

where: α_{2+}: ratio of the second mode contribution to the first mode contribution determined by Eq. (26).

$$\alpha_{2+} = \gamma_+ \cdot S_{A2}/S_{A1} \tag{26}$$

where: γ_+: coefficient expressing the phase of both first and second modes and it is assumed as unity in for its simplicity (Matsumori et al. 2002), and S_{A2} / S_{A1} is the ratio of response acceleration spectrum.

To simplify Eq. (26), another assumption is introduced as Eq. (27).

$$\alpha_{2+} = S_{A2}/S_{A1} = 1 \tag{27}$$

Note that Eq. (27) is valid only for the low-rise buildings with short predominant periods. Substituting Eq. (27) into Eq. (25), $\{f\}_+$ is obtained by simpler form as Eq. (28).
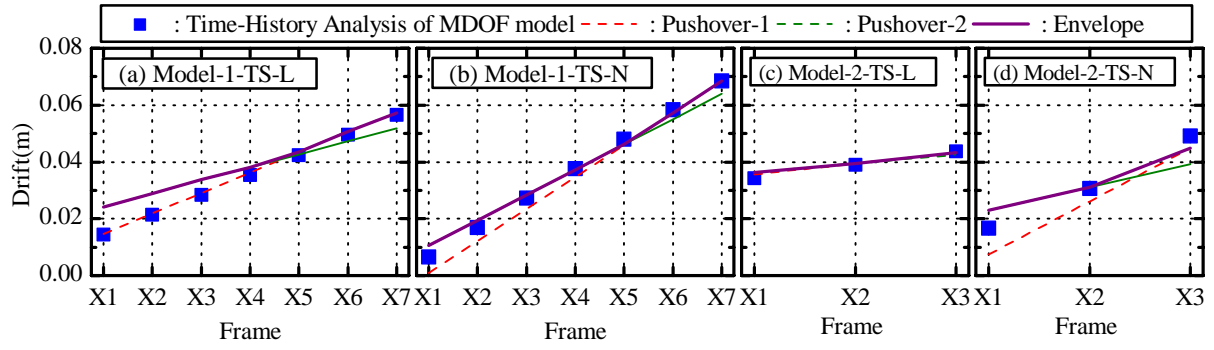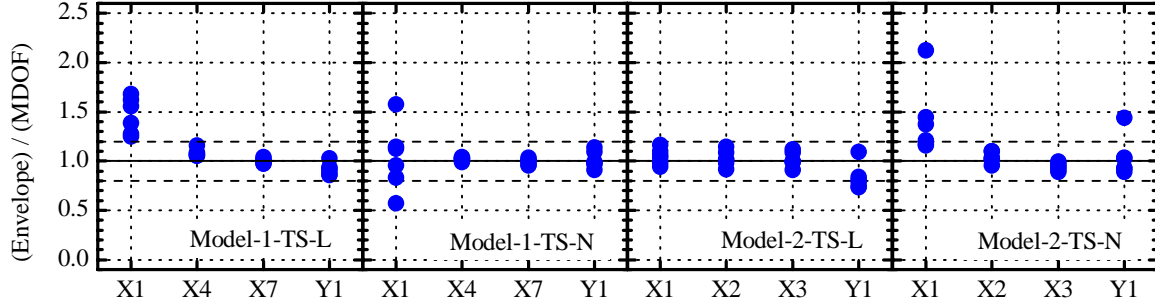
Fig. 22 Comparison of the drift in each frame

Fig. 23 Accuracy of the Equivalent SDOF model (TS Buildings)

$$\{f\}_+ = [M](\Gamma_1\{\phi_1\} + \Gamma_2\{\phi_2\}) = [M]\{\alpha\} \tag{28}$$

From assumptions expressed by Eqs.(26) and (27), $\{f\}_+$ is simplified as that the only lateral force is applied at C.M. as shown in Fig. 21(b), even if $\{\phi_1\}$ and $\{\phi_2\}$ vary in the nonlinear stage.

Fig. 22 shows the comparison of the drift in each frame obtained from time-history analysis of MDOF models subjected to TOH ground motion, predictions by the Pushover-1, and Pushover-2. This figure shows that the envelope of the results obtained by two different pushover analyses can approximate the results of time-history analysis of MDOF models. Fig. 23 shows the ratio of maximum drift at stiff-side frame (Frame X1 for both Model-1 and Model-2), center of mass (Frame X4 for Model-1 and Frame X2 for Model-2, respectively), flexible-side frame (Frame X7 for Model-1 and Frame X3 for Model-2, respectively) and the transverse frame (Frame-Y1 for both Model-1 and Model-2), predicted by the envelope of the two different pushover analyses and time-history analysis of MDOF model. This figure shows that the predictions at stiff-side frame are improved in Model-1-TS-N and Model-2-TS-N from the results shown in Fig. 10.

SIMPLIFIED NONLINEAR ANALYSIS PROCEDURE AND APPLICATION EXAMPLE

Based on the results obtained above, a simplified nonlinear analysis procedure for single-story asymmetric TS buildings is proposed.

Outline of the procedure

The outline of the proposed procedure is described as follows.

STEP 1: Pushover analysis of MDOF model
STEP 2: Determination of simplified equivalent SDOF model properties

STEP 3: Nonlinear dynamic analysis of simplified equivalent SDOF model
STEP 4: Estimation of drift demand in each frame of MDOF model

The procedure required in each step is described below.

STEP 1: A pushover analysis of a MDOF model is carried out to obtain the force - displacement relationship, considering the change in the first mode shape at each nonlinear stage described in Appendix B.

STEP 2: The equivalent acceleration A_1^*- displacement D_1^* relationship of the simplified equivalent SDOF model is determined from the results of **STEP 1**. Since the deformation shape $\{d\}$ having the first mode shape is imposed on the original model as described in **STEP 1**, A_1^* and D_1^* in Eq. (16) can be rewritten as Eq. (29).

$$D_1^* = \frac{\{d\}^T[M]\{d\}}{\{d\}^T[M]\{\alpha\}} = \left\{1+\left(\frac{r\cdot\theta}{y}\right)^2\right\}\cdot y, \quad A_1^* = \frac{\{d\}^T\{R\}}{\{d\}^T[M]\{\alpha\}} = \left\{1+\left(\frac{\theta}{y}\right)\cdot\left(\frac{T_Z}{V_Y}\right)\right\}\cdot\frac{V_Y}{m} \quad (29)$$

Then the A_1^*- D_1^* relationship is idealized by a tri-linear line so that the hysteretic energy dissipation enclosed by the original curve and the tri-linearly idealized line is same. In this study, the SDOF model idealized by a tri-linear curve is referred to as a "simplified equivalent SDOF model".

STEP 3: A nonlinear dynamic analysis of the simplified equivalent SDOF model is carried out to obtain the displacement demand $D_1^*{}_{MAX}$.

STEP 4: The drift in each frame of the original model based on the first mode response is determined from the results of **STEP 1** and **3**. By substituting $D_1^*{}_{MAX}$ obtained in **STEP 3** into Eq. (14), $\{d\}$ and hence the drift demand in each frame based on the first mode response can be found. Then, another pushover analysis is carried out using the sum of modal force distribution determined from Eq. (28) until D^* obtained by Eq. (24) reaches $D_1^*{}_{MAX}$. The drift demand in each frame of the original model is determined from the envelope of both pushover analyses.

Application examples

The nonlinear responses of TS buildings (Model-1-TS-L, Model-2-TS-L, and Model-1-TS-N, Model-2-TS-N) are estimated by the simplified procedure proposed above.

The correlation of drifts at the stiff-side frame, the center of mass and the flexible-side frame of each model obtained from the MDOF model and the simplified procedure are compared in Fig. 24. These figures show that the simplified procedure proposed herein successfully estimates the nonlinear responses of TS buildings.

<div align="center">

CONCLUSIONS

</div>

A simplified nonlinear analysis procedure to estimate the earthquake response of single-story asymmetric building is presented and its applicability is discussed. The major findings obtained in this study can be summarized as follows.

1) Single-story asymmetric buildings oscillate predominantly in the first mode when they are classified in torsionally stiff (TS) buildings, while their responses are influenced significantly by the second mode when they are classified in torsionally flexible (TF) buildings.
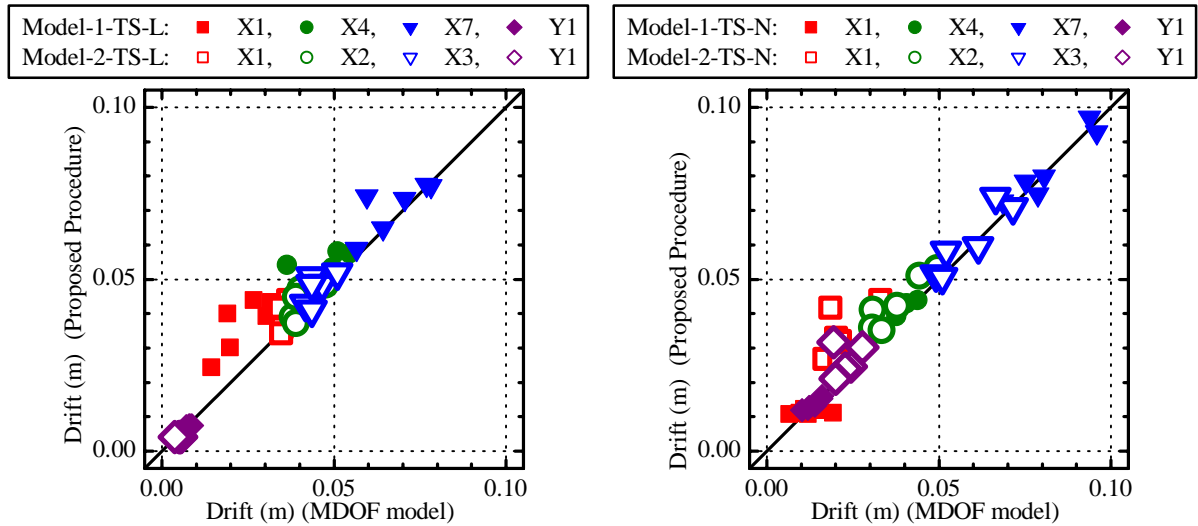
Fig. 24 Correlation of the maximum drift demand obtained proposed procedure and MDOF model

2) The equivalent SDOF model can be limitedly applied to TS buildings. To identify the TS building, the equivalent modal mass ratio m_1^* can be a good index.

3) It is essential to incorporate the change in the first mode shape to obtain more accurate responses of asymmetric buildings through the equivalent SDOF models.

4) The drift demand at stiff-side frame may be significantly underestimated by equivalent SDOF model due to the stiffness degradation of the transverse frames. To overcome this problem, the procedure using two different pushover analyses considering the first and second mode contribution is proposed. The predictions at stiff-side frame can be improved by the proposed procedure.

5) The response of TS buildings can be satisfactorily estimated by the simplified nonlinear analysis procedure proposed in this study. In TS buildings investigated in this paper, m_1^* is larger than 0.7, and the proposed procedure provides the satisfactory estimations.

The discussions in this paper are limited to single-story asymmetric buildings subjected to unidirectional ground motion. To extend the proposed procedure to a multi-story asymmetric building, however, it is most essential to develop a rational scheme to find its equivalent SDOF model. The extension of the procedure to a multi-story asymmetric building is the next phase of this study. And because the number of modes increases in case of multi-story asymmetric buildings, the equivalent modal mass ratio m_1^* may be smaller even if they oscillate predominantly in the first mode. Further study is needed to quantify the application limit of the equivalent SDOF model.

APPENDIX A. NONLINEAR ANALYSIS OF EQUIVALENT SDOF MODEL

The procedure for nonlinear analysis of equivalent SDOF model is summarized below in a step-by-step form:

18

1) Set a ground acceleration at next step $_{n+1}a_g$.

2) Assume the relative acceleration of equivalent SDOF model at the next step as $_{n+1}\ddot{D}_1 = {}_n\ddot{D}_1$.

3) Determine the first mode vector at the current step $_n\Gamma_1\{_n\phi_1\}$.

4) Assume the first mode vector at the next step as $_{n+1}\Gamma_1\{_{n+1}\phi_1\} = {}_n\Gamma_1\{_n\phi_1\}$.

5) Calculate the relative velocity $_{n+1}\dot{D}_1^*$ and the relative displacement $_{n+1}D_1^*$ of equivalent SDOF model at the next step by Eqs. (A1) and (A2).

$$_{n+1}\dot{D}_1^* = {}_n\dot{D}_1^* + \left(_n\ddot{D}_1^* + {}_{n+1}\ddot{D}_1^*\right)\cdot \Delta t/2 \tag{A1}$$

$$_{n+1}D_1^* = {}_nD_1^* + {}_n\dot{D}_1^* \cdot \Delta t + (1/2 - \beta)_n\ddot{D}_1^* \cdot \Delta t^2 + \beta\cdot_{n+1}\ddot{D}_1^* \cdot \Delta t^2 \tag{A2}$$

6) Calculate the displacement by equation (A3).

$$\{_{n+1}d\} = {}_{n+1}\Gamma_1\{_{n+1}\phi_1\}_{n+1}D_1^* \tag{A3}$$

7) Determine the deformation and restoring force of each element and calculate the restoring force $\{_{n+1}R\}$.

8) Determine the first mode shape $_{n+1}\Gamma_1\{_{n+1}\phi_1\}$ from the secant stiffness defined at the maximum deformation previously experienced.

9) Repeat steps 5) through 7) until $_{n+1}\Gamma_1\{_{n+1}\phi_1\}$ calculated in step 8) falls within an allowable band from the assumed first mode shape.

10) Calculate the equivalent mass $_{n+1}M_1^*$, the equivalent damping coefficient $_{n+1}C_1^*$, and the equivalent acceleration $_{n+1}A_1^*$ from Eqs. (A4) through (A6).

$$_{n+1}M_1^* = {}_{n+1}\Gamma_1^2\left(\{_{n+1}\phi_1\}^T[M]\{_{n+1}\phi_1\}\right) \tag{A4}$$

$$_{n+1}C_1^* = {}_{n+1}\Gamma_1^2\left(\{_{n+1}\phi_1\}^T[_{n+1}C]\{_{n+1}\phi_1\}\right) \tag{A5}$$

$$_{n+1}A_1^* = {}_{n+1}\Gamma_1\{_{n+1}\phi_1\}^T\{_{n+1}R\}/_{n+1}M_1^* \tag{A6}$$

11) Calculate the relative acceleration of equivalent SDOF model $_{n+1}\ddot{D}_1^*$ by Eq. (A7).

$$_{n+1}\ddot{D}_1^* = -_{n+1}a_g - \left(_{n+1}C_1^*/_{n+1}M_1^*\right)_{n+1}\dot{D}_1^* - {}_{n+1}A_1^* \tag{A7}$$

12) Repeat steps 4) through 11) until $_{n+1}\ddot{D}_1^*$ calculated in step 11) falls within the allowable band from the assumed relative acceleration.

APPENDIX B. PUSHOVER ANALYSIS PROCEDURE CONSIDERING THE CHANGE IN THE FIRST MODE SHAPE AT EACH NONLINEAR STAGE

The pushover analysis procedure considering the change in the first mode shape at each nonlinear stage is summarized below in a step-by-step form:

1) Set a displacement increment at the next step $_{n+1}\Delta y$.

2) Determine the first mode vector at the current step $_n\Gamma_1\{_n\phi_1\}$.

3) Assume the first mode vector at the next step as $_{n+1}\Gamma_1\{_{n+1}\phi_1\} = {}_n\Gamma_1\{_n\phi_1\}$.

4) Calculate the displacement by Eq. (A8).

$$\{_{n+1}d\} = {}_{n+1}\Gamma_1\{_{n+1}\phi_1\}_{n+1}D_1^* \tag{A8}$$

$$\text{where} \quad _{n+1}D_1^* = \left(_n y + {}_{n+1}\Delta y\right)/_{n+1}\Gamma_1 \tag{A9}$$

5) Determine the deformation and restoring force of each element.
6) Determine the first mode vector $_{n+1}\Gamma_1\{_{n+1}\phi_1\}$ from the secant stiffness defined at the maximum deformation previously experienced.
7) Repeat steps 4) through 6) until $_{n+1}\Gamma_1\{_{n+1}\phi_1\}$ calculated in step 6) falls within an allowable band from the assumed first mode shape.

REFERENCES

ATC-40 (1996). *Seismic evaluation and retrofit of concrete buildings*, *Vol. 1*, Applied Technology Council, Redwood City, USA.

Azuhata T, Saito T, Takayama M, Nagahara K. (2000). "Seismic performance estimation of asymmetric buildings based on the capacity spectrum method", *Proceedings of Twentieth World Conference on Earthquake Engineering*, CD-ROM.

Fajfar P. (2000). "A nonlinear analysis method for performance-based seismic design", *Earthquake Spectra*, Vol.16, No. 3, 573-592.

Fajfar P. (2002). "Structural analysis in earthquake engineering – a breakthrough of simplified non-linear methods", *Proceeding of Twentieth European Conference on Earthquake Engineering,* CD-ROM.

FEMA-273 (1997). *NEHRP guidelines for the seismic rehabilitation of buildings*, Building Seismic Safety Council, developed by ATC for FEMA, Washington, D.C., USA.

Kan, CL, Chopra, AK. (1977). "Effects of torsional coupling on earthquake forces in buildings", *Journal of the Structural Division*, Vol. 103, No. ST4, ASCE, 805-819.

Kilar V, Fajfar P. (2001). "On the applicability of pushover analysis to the seismic performance evaluation of asymmetric buildings", *European Earthquake Engineering*, Vol.15, No.1, 20-31.

Kuramoto H, Teshigawara M, Okuzono T, Koshika N, Takayama M, Hori T. (2000). "Predicting the earthquake response of buildings using equivalent single degree of freedom system", *Proceedings of Twentieth World Conference on Earthquake Engineering*, CD-ROM.

Matsumori T, Otani S, Shiohara H, Kabeyasawa T, (2002). "Estimation of earthquake maximum response of R/C frame structures using nonlinear static analysis*", Summaries of Technical Papers of Annual Meeting*, Architectural Institute of Japan, C-2, 885-886 (in Japanese).

Moghadam AS, Tso WK. (1996). "Damage assessment of eccentric multistory buildings using 3-D pushover analysis", *Proceedings of Eleventh World Conference on Earthquake Engineering*, CD-ROM

Moghadam AS, Tso WK. (1998). "Pushover analysis for asymmetrical multistorey buildings", *Proceedings of the Sixth U.S. National Conference on Earthquake Engineering*, CD-ROM.

Ohami K, Murakami M. (2000). "Indices of effects of torsional of torsional coupling on earthquake response of structures", *Proceedings of Twentieth World Conference on Earthquake Engineering*, CD-ROM

Saiidi M, Sozen MA. (1981). "Simple nonlinear seismic analysis of R/C structures", *Journal of the Structural Division*, Vol. 107, ST5, ASCE, 937-952

Takeda T, Sozen MA, Nielsen NN. (1970). "Reinforced concrete response to simulated earthquakes", *Journal of the Structural Division*, Vol. 96, No. ST12, ASCE, 2557-2573

Yamazaki Y. (1988). "Lateral torsional response of buildings during earthquakes", *Proceedings of Ninth World Conference on Earthquake Engineering*, Vol. V, 73-78.